Theoretical modeling of fiber laser at 810 nm based on thulium-doped silica fibers with enhanced 3H4 level lifetime

Pavel Peterka, Ivan Kašík, Anirban Dhar, Bernard Dussardier, Wilfried Blanc

Theoretical modeling of fiber laser at 810 nm based on thulium-doped silica fibers with enhanced $^3H_4$ level lifetime

Pavel Peterka,[1,*] Ivan Kasik,[1] Anirban Dhar,[1,3] Bernard Dussardier,[2] and Wilfried Blanc[2]

[1]Institute of Photonics and Electronics ASCR, v.v.i., 18251 Prague, Czech Republic
[2]Laboratoire de Physique de la Matière Condensée, Université de Nice-Sophia-Antipolis, CNRS UMR 6622 Avenue Joseph Vallot, Parc Valrose, 06108 NICE CEDEX 2, France
[3]Now with Optoelectronic Research Centre, University of Southampton, Southampton, SO17 1BJ, UK
**peterka@ufe.cz*

Abstract: A compact upconversion fiber laser operating around 810 nm is proposed using thulium-doped silica-based fiber with locally modified thulium environment by high alumina codoping. Using a comprehensive numerical model of thulium doped fiber we investigate performance of the proposed laser. Comparison with two other thulium hosts, fluoride glass and standard silica, is presented. Efficient lasing can be expected even for silica based fiber for specific ranges of the fiber and laser cavity parameters, especially when $^3H_4$ lifetime is enhanced. With moderate pump power of 5 W at wavelength of 1064 nm, the predicted output power of the upconversion laser is about 2 W at 810 nm.

OCIS codes: (140.3510) Lasers, fiber; (140.3613) Lasers, upconversion.

References and links

1. S. Ohara, N. Sugimoto, Y. Kondo, K. Ochiai, Y. Kuroiwa, Y. Fukasawa, T. Hirose, H. Hayashi, and S. Tanabe, "Bi_2O_3-based glass for S-band amplification," Proc. SPIE **4645**, 8–15 (2002).
2. M. L. Dennis, and B. Cole, "Amplification device utilizing thulium doped modified silicate optical fiber," US patent No. 6,924,928 B2, August 2 (2005).
3. P. R. Watekar, S. Ju, and W. T. Hu, "A Nd-YAG laser-pumped Tm-doped silica glass optical fiber amplifier at 840 nm," IEEE Photon. Technol. Lett. **18**(15), 1651–1653 (2006).
4. B. Faure, W. Blanc, B. Dussardier, and G. Monnom, "Improvement of the Tm^{3+}:$^3H_4$ level lifetime in silica optical fibers by lowering the local phonon energy," J. Non-Cryst. Solids **353**(29), 2767–2773 (2007).
5. W. Blanc, T. L. Sebastian, B. Dussardier, C. Michel, B. Faure, M. Ude, and G. Monnom, "Thulium environment in a silica doped optical fibre," J. Non-Cryst. Solids **354**(2-9), 435–439 (2008).
6. P. Peterka, I. Kasik, A. Dhar, B. Dussardier, and W. Blanc, "Theoretical analysis of fiber lasers emitting around 810 nm based on thulium-doped silica fibers with enhanced $^3H_4$ level lifetime", In Europhysics Conference Abstracts **34C**, 4th EPS-QEOD Europhoton conference, Germany, WeP5 (2010).
7. J. N. Carter, R. G. Smart, A. C. Troper, D. C. Hanna, S. F. Carter, and D. Szebesta, "Theoretical and experimental investigation of a resonantly pumped thulium doped fluorozirconate fiber amplifier at around 810 nm," J. Lightwave Technol. **9**(11), 1548–1553 (1991).
8. I. Bufetov, and E. M. Dianov, "Bi-doped fiber lasers," Laser Phys. Lett. **6**(7), 487–504 (2009).
9. M. L. Dennis, J. W. Dixon, and I. Aggarwal, "High power upconversion lasing at 810 nm in Tm:ZBLAN fibre," Elctron. Lett. **30**(2), 136–137 (1994).
10. P. R. Watekar, S. Ju, and W. T. Hu, "800-nm upconversion emission in Yb-sensitized Tm-doped optical fiber," IEEE Photon. Technol. Lett. **18**(15), 1609–1611 (2006).
11. D. A. Simpson, W. E. Gibbs, S. F. Collins, W. Blanc, B. Dussardier, G. Monnom, P. Peterka, and G. W. Baxter, "Visible and near infra-red up-conversion in Tm^{3+}/Yb^{3+} co-doped silica fibers under 980 nm excitation," Opt. Express **16**(18), 13781–13799 (2008), http://www.opticsinfobase.org/oe/abstract.cfm?URI=oe-16-18-13781.
12. A. Pal, A. Dhar, S. Das, S. Y. Chen, T. Sun, R. Sen, and K. T. V. Grattan, "Ytterbium-sensitized Thulium-doped fiber laser in the near-IR with 980 nm pumping," Opt. Express **18**(5), 5068–5074 (2010), http://www.opticsinfobase.org/oe/abstract.cfm?URI=oe-18-5-5068.
13. M. Grinberg, D. L. Russell, and K. Holliday, "Continuous function decay analysis of a multisite impurity activated solid," Opt. Commun. **156**(4-6), 409–418 (1998).
14. P. Peterka, B. Faure, W. Blanc, M. Karasek, and B. Dussardier, "Theoretical modelling of S-band thulium-doped silica fibre amplifiers," Opt. Quantum Electron. **36**(1-3), 201–212 (2004).

#137903 - $15.00 USD Received 9 Nov 2010; revised 14 Jan 2011; accepted 21 Jan 2011; published 28 Jan 2011

15. W. Blanc, P. Peterka, B. Faure, B. Dussardier, G. Monnom, I. Kasik, J. Kanka, D. Simpson, and G. Baxter, "Characterization of thulium-doped silica-based optical fibre for S-band amplifier," Proc. SPIE **6180**, 61800V–1, 61800V-6 (2006).
16. S. D. Jackson, and T. A. King, "Theoretical modeling of Tm-doped silica fiber lasers," J. Lightwave Technol. **17**(5), 948–956 (1999).
17. T. Komukai, T. Yamamoto, T. Sugawa, and Y. Miyajima, "Upconversion pumped thulium-doped fluoride fiber amplifier and laser operating at 1.47 um," IEEE J. Quantum Electron. **31**(11), 1880–1888 (1995).
18. P. Peterka, I. Kasik, V. Matejec, W. Blanc, B. Faure, B. Dussardier, G. Monnom, and V. Kubecek, "Thulium-doped silica-based optical fibers for cladding-pumped fiber amplifiers," Opt. Mater. **30**(1), 174–176 (2007).
19. E.-G. Neumann, *Single mode fibers* (Springer Verlag, Berlin, 1988) Chap. 6.3.
20. P. Peterka, I. Kasik, A. Dhar, B. Dussardier, and W. Blanc, "Thulium-doped silica fibers with enhanced $^3H_4$ level lifetime: modelling the devices for 800-820 nm band," Proc. SPIE **CDS417** (to be published).
21. J. Chen, X. Zhu, and W. Sibbett, "Rate-equation studies of erbium-doped fiber lasers with common pump and laser energy bands," J. Opt. Soc. B **9**(10), 1876–1882 (1992).

1. Introduction

Most reliable operating wavelengths offered by rare-earth doped fiber devices are situated around 1, 1.5 and 2 μm by using ytterbium, erbium and thulium-doped fibers (TDFs), respectively. The thulium ions offer other laser transitions but they are usually less attractive mainly because of relatively low quantum conversion efficiency of the respective upper laser levels in high-phonon energy silica-based fibers. Efficient operation of TDF based devices can be easily reached in low-phonon energy host like fluoride based fibers. However, usage of fluoride fibers results in difficulties with fabrication, hygroscopicity and aging of the host material and low pump power damage threshold. These complications spurred development of alternative host materials with reduced phonon energy that possess long-term reliability. Intended applications were mainly aimed at amplifiers for the telecommunication S-band (1460-1530 nm). Local modification of the thulium environment belongs to promising approaches, e.g., by codoping the fiber core with oxides of bismuth [1] and gallium or germanium [2, 3]. We have shown that with modification of local environment of the thulium ions by alumina, the quantum conversion efficiency of transition originating from the thulium $^3H_4$ level is about four times increased compare to pure silica host [4, 5].

In this article, we investigate different application of silica-based TDF: the fiber lasers operating around 810 nm that would extend the spectral range covered by high-power fiber devices. To our knowledge, silica-based thulium-doped fibers have not been used in high-power fiber lasers at around 800 nm and neither such device has been theoretically analyzed yet. The article is based on our preliminary results presented in a conference paper [6]. Several theoretical and experimental studies have been already done for TDF amplifiers for the 800-850 spectral region, mainly in fluoride fiber host [7] and recently also in silica host [3]. The single-transverse mode, high-power lasers in this spectral band can be used for fiber sensors, instrument testing and for pumping of special types of lasers and amplifiers. Particularly, bismuth-doped fibers pumped around 800 nm may shift their gain to 1300 nm telecommunication band, where highly reliable silica-based fiber amplifiers are still unavailable [8]. An efficient fiber laser in 800 nm spectral region could potentially be used as a replacement for titanium sapphire laser in some applications. Amplification and lasing at around 810 nm has already been investigated using low-phonon energy fluoride-based TDFs that exhibit high quantum efficiency of the upper laser level $^3H_4$. Output power of up to 2 W and 37% slope efficiency was achieved in fluoride-fiber host [9]. The output power was limited by low-pump power damage threshold of the fluoride fiber. In the same laboratory, they observed also lasing action at 803 nm in thulium-doped silica-based fibers that they were studying for amplification in the telecommunication S-band [2], but the details about the actual output power characteristics were not reported. To our knowledge, it is the only experimental laser demonstration of the thulium transition $^3H_4 \rightarrow {}^3H_6$ in a silica fiber. It should be noted that although the laser diodes at this wavelength have been available for a long time, commercially available single-mode laser diodes are limited to about 200 mW of output power in diffraction limited beam.

#137903 - $15.00 USD Received 9 Nov 2010; revised 14 Jan 2011; accepted 21 Jan 2011; published 28 Jan 2011

2. Fiber laser setup and fiber characteristics

Two fiber laser setups were investigated. The first one utilizes upconversion pumping scheme shown in Fig. 1a and has a compact all-fiber setup, example of which is shown in Fig. 1c. Ytterbium-doped fiber laser may serve as reliable and inexpensive pump sources. However, pumping at single wavelength at around 1060 nm would lead to unwanted second step of excited-state absorption (ESA) to the $^1G_4$ level. In addition, promotion of thulium ions to even higher laying states becomes more probable. This might lead to color center formation and consequently to photodarkening. Therefore, we propose also an alternative pumping scheme, see Fig. 1b, and laser setup, see Fig. 1d, that would not lead to excitation of the $^1G_4$ level and that should allow experimental study of the proposed applications effectively mitigating photodarkening. Both proposed setups utilize core-pumping.

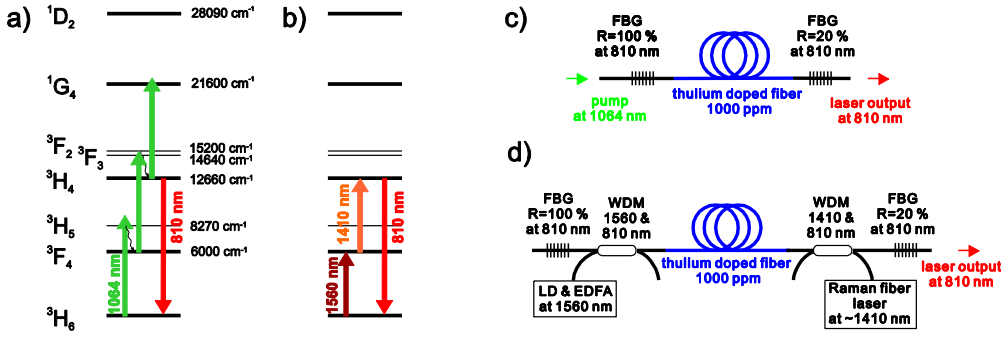

Fig. 1. Thulium energy level diagrams with depicted (a) single- and (b) dual-wavelengths upconversion pumping schemes and the corresponding TDF laser setups for (c) single- and (d) dual-wavelength pumping.

Potentially, the TDFs co-doped with ytterbium may open the possibility for cladding pumping [10–12]. The thulium-doped fiber was drawn from preform fabricated by using the MCVD (Modified Chemical Vapor Deposition) and solution doping methods. From fiber attenuation we determined that the concentration of thulium was 40 ppm mol. The concentrations of GeO_2 and alumina were measured by electron microprobe analysis to be up to 4 and 10 mol %, respectively. The background loss of 0.1 dB/m was measured at 850 nm. The $^3H_4$ lifetime of 58 μs was measured. Since the decay curve was not possible to fit with a single exponential, the lifetime used in the numerical model was approximated by the value of the time interval in which the fluorescence dropped to the 1/e of its peak value. We have studied the non-exponential shape of thulium ions fluorescence in a previous paper [5]. It is not due to energy transfers among thulium ions or from a thulium ion to an OH radical. It was clearly related to presence of Tm^{3+} ions in different environments. Indeed, the 0.8 μm-emission band corresponds to the transition between the two excited levels $^3H_4$ and $^3H_6$. The $^3H_4$ lifetime is affected by a non-radiative emission which occurs from the $^3H_4$ level to the $^3H_5$ level directly located below the emitting level. The probability of this transition depends exponentially on the energy gap and the maximum phonon energy (MPE). In alumina-doped silica-based fibers, we have demonstrated that thulium ions are located both in almost pure silica environment (MPE=1100 cm^{-1}) and in alumina-rich sites (MPE=780 cm^{-1} for aluminates). The non-exponential shape of the decay curves was then explained by considering a multitude of different sites available for the rare-earth ion, leading to a multitude of decay constants. This phenomenological model was first proposed by Grinberg *et al.* [13].

#137903 - $15.00 USD Received 9 Nov 2010; revised 14 Jan 2011; accepted 21 Jan 2011; published 28 Jan 2011

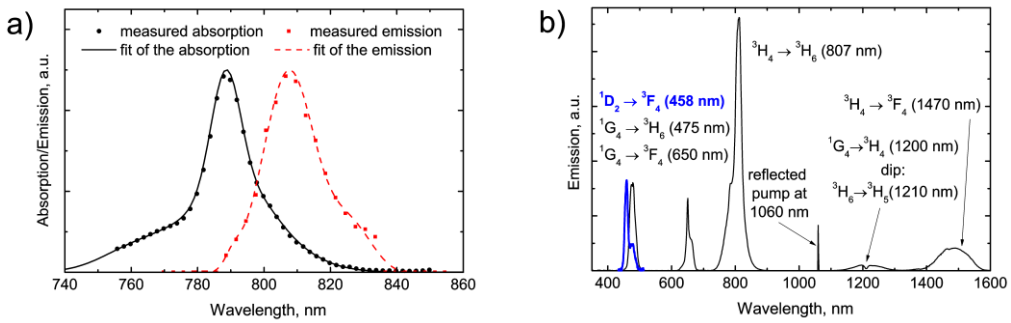

Fig. 2. (a) Detail of the emission and absorption spectra around 800 nm of the TDF under test. (b) Backward emission of the TDF pumped by 500 mW at 1060 nm (thin black line). The thick blue line represents the change in the emission in the blue part of the spectrum when another 300 mW of pump at around 1440 nm was added.

The absorption and emission spectra around 800 nm were measured, see Fig. 2a. The visible and near infrared emission spectra of the thulium doped fiber under study pumped with 500 mW at 1060 nm by ytterbium fiber laser is depicted by thin line in Fig. 2b. The blue peak at 475 nm corresponds to the $^1G_4 \rightarrow {}^3H_6$ transition. The other blue peak at 458 nm (thick blue line in Fig. 2b) due to the $^1D_2 \rightarrow {}^3F_4$ transition was observed when excitation sources at 1430 & 1440 & 1450 nm (300 mW in total) were added. It can be inferred from this spectral line shift that the upconversion processes from the $^1G_4$ level are weak for the pump wavelength of about 1060 nm.

3. Theoretical model

The diagram of thulium-ion energy levels is shown in Fig. 3 with all transitions involved in the model. The levels $^3F_2$ and $^3F_3$ are very close and they are treated as single level No. 4. The stimulated absorption and emission rates W_{ij} account for amplified spontaneous emission (ASE). Spontaneous decay processes are described by A_{ij} and $A^{nr}{}_i$, the radiative and nonradiative decay rates, respectively.

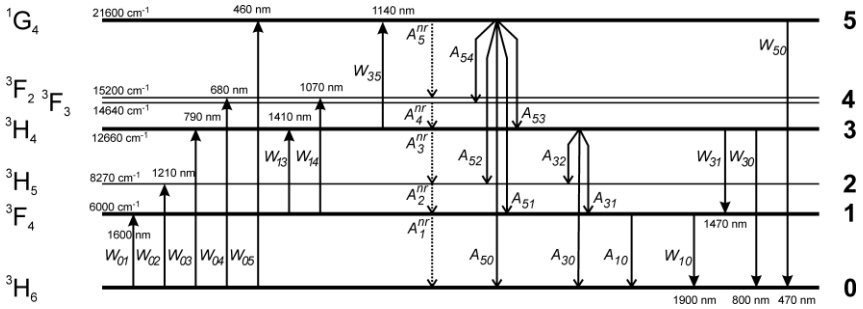

Fig. 3. Thulium energy level diagram with transitions involved in the theoretical model.

The population densities of thulium ions N_2 and N_4 are neglected, because the nonradiative decay rates from the $^3F_{2,3}$ and $^3H_5$ levels are very high (>> 10^5 s^{-1}). According to the energy level diagram in Fig. 3, we can write time-dependent differential rate equations for the population density in the relevant excited levels N_1, N_3, and N_5:

$$\frac{dN_1}{dt} = N_0(W_{01}+W_{02}) - N_1(W_{10}+W_{13}+W_{14}+A_1^{nr}+A_{10}) + \\ + N_3(W_{31}+A_3^{nr}+A_{32}+A_{31}) + N_5(A_{51}+A_{52}), \quad (1)$$

#137903 - $15.00 USD Received 9 Nov 2010; revised 14 Jan 2011; accepted 21 Jan 2011; published 28 Jan 2011

$$\frac{dN_3}{dt} = N_0(W_{03}+W_{04}) + N_1(W_{13}+W_{14}) + N_5(A_5^{nr}+A_{54}+A_{53}) - \\ - N_3\left(W_{35}+W_{31}+W_{30}+A_3^{nr}+\sum_{j=0}^{2}A_{3j}\right), \tag{2}$$

$$\frac{dN_5}{dt} = N_0W_{05} + N_3W_{35} - N_5(W_{50}+A_5^{nr}+\sum_{j=0}^{4}A_{5j}), \tag{3}$$

while it holds:

$$N_t = N_0 + N_1 + N_3 + N_5, \tag{4}$$

where N_t is concentration of thulium ions in the fiber core. Under steady state conditions, the rate equations transfer to four linear algebraic equations. The propagation of optical power of the signals, the pumps and the ASE are governed by first order differential equations, so called propagation equations:

$$\frac{dP^{\pm}(\lambda)}{dz} = \pm\Gamma(\lambda)P^{\pm}(\lambda)\sum_{ij}^{\{10,30,31,50\}}\left(N_i\sigma_{ij}(\lambda) - N_j\sigma_{ji}(\lambda)\right) \\ \mp\Gamma(\lambda)P^{\pm}(\lambda)\left(N_0\sigma_{02}(\lambda)+N_0\sigma_{04}(\lambda)+N_1\sigma_{14}(\lambda)+N_3\sigma_{35}(\lambda)\right) \\ \pm\Gamma(\lambda)\sum_{ij}^{\{10,30,31,50\}}2M(\lambda)h\nu_{ij}\Delta\nu N_i\sigma_{ij}(\lambda)\mp\alpha(\lambda)P^{\pm}(\lambda), \tag{5}$$

where σ_{ij} is the respective transition cross section, h is Planck's constant, Γ is the overlap factor that accounts for mutual overlap of the electromagnetic field with the rare-earth ions, M is number of modes that can propagate in the fiber at specific λ and finally α is the background loss. The power P^+ represents power of an optical wave that propagates in the same direction as the pump at 1060 nm in Fig. 1c or the pump at 1560 nm in Fig. 1d. The upper index P^- denotes optical power propagating in opposite direction. Evolution of optical power in each ASE spectral slot around a wavelength λ (typical width of such a partial wave is 1 nm) is governed by its respective propagation equation. The first term in Eq. (5) describes the amplification and reabsorption of optical signals, the second term represents ground-state absorption (GSA) and ESA in spectral bands with no significant emission, the third term accounts for spontaneous emission and the fourth term stands for background loss of the fiber. The details about definition of overlap factor and transition rates can be found in [14]. Spectral dependence of the cross-sections σ_{ij} is shown in Fig. 4. The emission and absorption spectra are taken from Ref [14] apart from the spectra of the $^3H_6 \leftrightarrow {}^3H_4$ transition that are taken in accordance with Fig. 2a. The cross sections are fitted with a linear combination of Gaussian functions:

$$\sigma(\lambda) = \sum_{k=1}^{4} a_k \exp\left[-2\left(\frac{\lambda-\lambda_k}{\Delta\lambda_k}\right)^2\right] \tag{6}$$

The peak values a_k, central wavelengths λ_k and full widths at half maximum $\Delta\lambda_k$ are listed in Table 1. The list contains the transitions where the spectral dependence is of great importance in the presented modeling. The propagation Eqs. (5) for all partial waves, together with the set of the rate Eqs. (1-4) under steady state conditions, are solved simultaneously along the fiber using Runge-Kutta-Gill method of the fourth order. Since the boundary conditions for the counterpropagating partial waves P^- are not known at the beginning of the fiber (z = 0), an iterative process must be applied. The described numerical model of thulium-doped fiber was validated by comparison with measurement of the amplification of a signal from the telecommunication S-band [15].

#137903 - $15.00 USD Received 9 Nov 2010; revised 14 Jan 2011; accepted 21 Jan 2011; published 28 Jan 2011

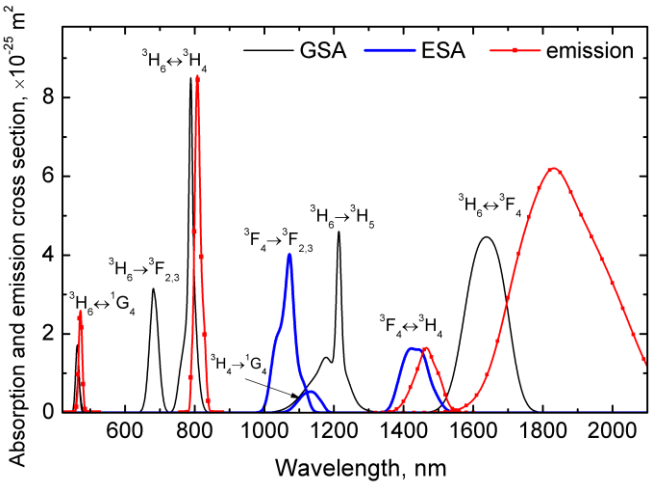

Fig. 4. Thulium absorption and emission cross-section spectra used in the model.

Table 1. Coefficients of best fits of absorption and emission spectra

transition:	$^3H_6 \rightarrow {}^3H_4$	$^3H_4 \rightarrow {}^3H_6$	$^3F_4 \rightarrow {}^3F_{2,3}$	$^3H_4 \rightarrow {}^1G_4$	$^3H_6 \rightarrow {}^3H_5$	$^3F_4 \rightarrow {}^3H_4$	$^3H_4 \rightarrow {}^3F_4$	$^3H_6 \rightarrow {}^3F_4$	$^3F_4 \rightarrow {}^3H_6$
λ_1[nm]	760.71	790.80	1072.0	1145.0	1171.2	1392.2	1462.2	1677.7	1741.9
$\Delta\lambda_1$[nm]	20.593	4.862	31.160	28.785	28.895	36.007	71.884	68.954	124.26
a_1[× 10^{-25} m^2]	0.81627	0.06277	3.3505	0.39585	0.38737	0.72574	0.66982	2.5593	1.7845
λ_2[nm]	788.58	807.564	1111.7	1167.2	1177.2	1419.3	1455.9	1612.9	1831.9
$\Delta\lambda_2$[nm]	8.9790	15.414	27.251	19.399	28.895	34.648	66.571	84.664	76.661
a_2[× 10^{-25} m^2]	5.2780	0.96849	0.66423	0.11809	0.38737	1.18050	0.55496	3.7476	0.6911
λ_3[nm]	799.13	826.07	1073.4	1120.0	1214.0	1451.9	1467.0	-	2018.5
$\Delta\lambda_3$[nm]	10.862	13.201	12.131	30.242	13.355	34.600	27.130	-	158.19
a_3[× 10^{-25} m^2]	0.42233	0.22652	0.56860	0.33098	3.467	1.20470	0.43041	-	1.5267
λ_4[nm]	789.86	-	1034.6	1097.1	1227.9	1484.2	1502.3	-	1856.5
$\Delta\lambda_4$[nm]	29.683	-	32.086	35.306	39.904	42.505	30.051	-	202.28
a_4[× 10^{-25} m^2]	3.1563	-	1.7087	0.19601	0.51216	0.46263	0.36261	-	4.9382

4. Results of numerical modeling

For predicting the performance of various thulium doped fiber devices and their optimization, we used the numerical model described above. To reduce the length of the TDF, thulium ion concentration is set to 1000 ppm mol for numerical simulations as the pair-induced quenching processes among neighboring thulium ions can still be assumed negligible at this concentration level [16]. Cumulated cavity losses of 1 dB due to insertion losses of splices and components are assumed. The fluorescence lifetimes of the relevant thulium energy levels in the three host materials are summarized in Table 2.

Table 2. Fluorescence lifetimes of thulium energy levels in three different fiber hosts.The values are given in µs.

Tm energy level	$^3F_4$	$^3H_4$	$^1G_4$
ZBLAN [17]	9000	1350	1110
modified silica (with high-alumina content) [15,18]	430	58	540
standard silica [16]	334.7	14.2	783.9

#137903 - $15.00 USD Received 9 Nov 2010; revised 14 Jan 2011; accepted 21 Jan 2011; published 28 Jan 2011

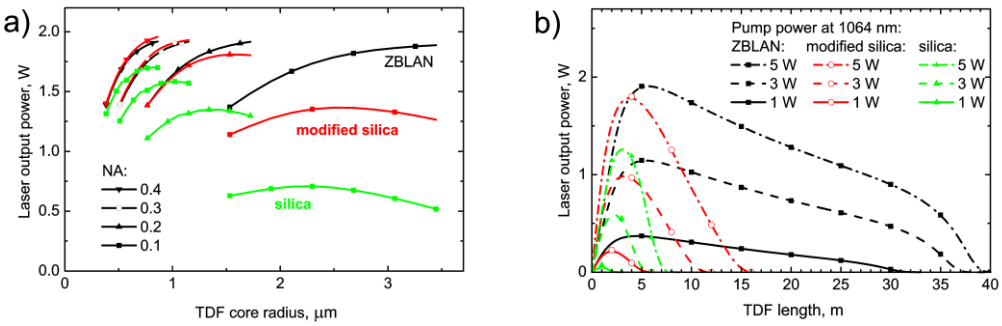

Fig. 5. (a) Laser output power at 810 nm vs. fiber core radius for several values of NA and pump power of 5 W at 1064 nm. (b) Laser output at 810 nm vs. TDF length for three different host materials and three pump power levels.

Intentionally, we kept the thulium cross sections identical for all three hosts to allow for comparison of the three materials in terms of the effect of their local phonon energy to the laser output. Although the three different materials differ slightly also in the other spectroscopic properties, namely branching ratios and radiative lifetimes of the respective energy levels, we have checked that the results of numerical modeling are almost exclusively influenced by the fluorescence lifetimes, especially the $^3H_4$ fluorescence lifetime.

We have optimized the fiber (core radius - *a*, numerical aperture - *NA*, radius of doping with thulium) and cavity (reflectivity of the output mirror, TDF length) parameters according to the most simple and compact setup (Fig. 1c). In general, the laser slope may not be constant with increasing pump power due to gradual populating of the $^1G_4$ level. Therefore, for a given pump power all the parameters of the fiber and laser cavity were optimized for maximal output power at the optimum fiber length. The output power was found weakly sensitive to the output fiber Bragg grating (FBG) reflectivity in the 70-95% range, therefore we chose 80% reflectivity of the output FBG in further modeling of the laser. The dependence of the output power of the laser at 810 nm on fiber core radius is shown in Fig. 5a for several values of *NA* and for the three fiber hosts. The range of relevant core radii is limited to the interval of single-mode regime at the laser wavelength, i.e., where the expected effective cutoff wavelength is smaller than 800 nm. Please note that for the effective cutoff wavelength λ_{ce} the normalized frequency $V=(2\pi/\lambda_{ce})aNA$ is about 2.8 and not 2.405 as it is in the case of the so-called theoretical cut-off wavelength [19]. The output power increases with increasing *NA*, but the enhancement becomes less significant above *NA*=0.2. Since fabrication of TDF with higher *NA* may pose difficulties, we restricted further studies to fibers with *NA*=0.2 as a compromise. The output powers level does not vary significantly for $a>1.4$ μm for *NA*=0.2. Since larger core would facilitate low-loss splicing with passive fibers, the core radius close to the larger limit (a=1.7 μm) is assumed in the following calculations. Detailed investigations of these TDF parameters on the laser performance shall be found in [20].

The optimum length of the TDF can be determined from the calculated dependence of the laser output on the TDF length as it is shown in Fig. 5b for the three laser hosts and three different pump power levels. The optimum TDF parameters mentioned above were used in the calculations and the background loss of 0.1 dB/m was considered. It can be seen in Fig. 5b that lasing at 810 nm is hard to achieve with silica based Tm-doped fiber in contrast to the fluoride host materials. However, the lasing might be possible even for silica based fiber for specific short range of the fiber lengths. Especially when the $^3H_4$ lifetime is enhanced, the laser output is very close to the one of ZBLAN host. Indeed, with optimized TDF waveguide parameters and length, the slope efficiency of the upconversion fiber laser would be similar for all three hosts. This result is similar to the well known case of the two-level fiber laser, where the laser rate equations and propagation equations can be solved analytically and the formulae for the laser threshold and slope efficiency are known [21]. In the two level laser system the laser threshold depends on the fluorescence lifetime of the upper laser level but the

#137903 - $15.00 USD Received 9 Nov 2010; revised 14 Jan 2011; accepted 21 Jan 2011; published 28 Jan 2011

laser slope does not. Although the upconversion pumped laser cannot be described by the simple two-level model, the trends are similar, at least for the optimized TDF and laser cavity parameters.

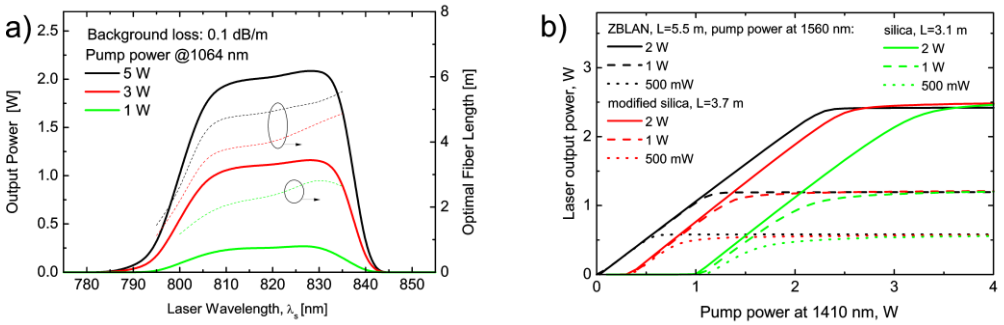

Fig. 6. (a) Laser wavelength tuning characteristics. (b) Examples of the dual-wavelength pumped upconversion laser. The output power at 810 nm is plotted vs. the pump power at 1410 nm (ESA $^3F_4 \rightarrow {}^3H_4$) for the three different host materials and for three pump power levels at 1560 nm (ground state absorption $^3H_6 \rightarrow {}^3F_4$).

We explored also the tunability of the TDF laser with the modified silica host. In this case we have measured the actual absorption and emission spectra around 800 nm as shown in Fig. 2a. With the measured absorption and emission spectra and for given laser cavity parameters the laser output vs. wavelength of the FBGs is shown in Fig. 6a. The tunability of the laser of more than 30 nm is expected.

As an example of the dual wavelength pumped, upconversion fiber laser according to Fig. 1b and 1d we have calculated the laser output at 810 nm vs. pump power for the three fiber hosts, see Fig. 6b. Since the optimization issues of the dual-wavelength pumping scheme are beyond the scope of this article, we have chosen the same TDF laser parameters that were used in Fig. 5b. The optimum TDF lengths according to Fig. 5b at power level of 5 W were considered for the respective materials. Since the second ESA to the $^1G_4$ level is not present in such a pumping scheme, and because of the lower quantum defect between the pump and the signal photons, the power conversion efficiency is higher than in the simple and compact setup with only one pump laser. Another important difference between the dual- and single-wavelength pumping schemes is that the signal output power does not increase with increasing the pump at only one pump wavelength. Beyond certain pump power at 1410 nm the laser output does not increase because of deficiency of thulium ions excited to the $^3F_4$ level. On the other hand, the pump power at 1560 nm must be kept lower than the pump at 1410 nm for the ESA to prevent buildup of the ASE around 2 μm that will result in significant deterioration of the pump conversion efficiency. Therefore, the pump power distribution among both wavelengths must be carefully balanced, as shown in Fig. 7a. In this figure, we calculated the laser output power at 810 nm and ASE in the 2 μm spectral region as a function of the ratio of pump power at 1560 nm to pump power at 1410 nm. The pump at 1410 nm should be higher because the lifetime of $^3H_4$ level is almost an order of magnitude shorter than the lifetime of $^3F_4$ level. This effect is pronounced especially for lower total pump powers. With increasing total pump power the optimum ratio of pump powers approaches the ratio of energies of the two photons that are necessary for the upconversion pumping to the $^3H_4$ level. Both pump transitions $^3H_6 \rightarrow {}^3F_4$ and $^3F_4 \rightarrow {}^3H_4$ exhibit relatively large spectral bandwidth, see Fig. 4. As a consequence, the laser performance depends only little on the potential wavelength instabilities of the pump lasers. The pump wavelengths can be selected within broad bands of 1530-1700 nm and 1390-1470 nm for the pump transitions $^3H_6 \rightarrow {}^3F_4$ and $^3F_4 \rightarrow {}^3H_4$, respectively, as shown in Fig. 7b. Nevertheless it should noted that the necessity of two different pump sources and more complex setup makes this pumping scheme

#137903 - $15.00 USD Received 9 Nov 2010; revised 14 Jan 2011; accepted 21 Jan 2011; published 28 Jan 2011

less attractive. The importance of the dual wavelength pumping scheme lies mainly in laboratory tests where the possible photodarkening should be effectively mitigated.

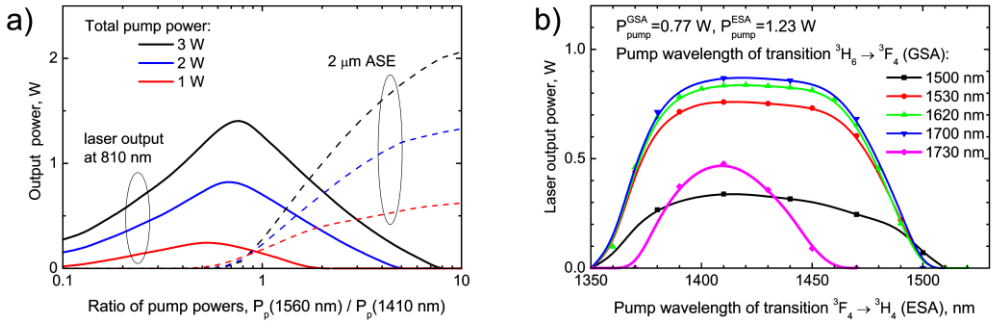

Fig. 7. (a) Laser output at 810 nm and total power of the ASE originated from the $^3F_4$ level vs. ratios of pump power at 1560 and 1410 nm. (b) Dependence of the laser output on the pump laser wavelengths.

4. Conclusions

We have proposed compact and simple thulium-doped silica fiber laser with a possible high-power output at 810 nm. To our knowledge, we have presented the first analysis of such fiber lasers as neither silica-based thulium-doped fibers have been used in high-power fiber lasers at around 800 nm, nor such device has been theoretically analyzed yet. We have proposed two different pumping schemes. The simpler one uses only single-wavelength pumping at around 1060 nm and the second one uses two wavelengths at around 1560 and 1410 nm. The second pumping scheme is advantageous in terms of mitigating the possible photodarkening by avoiding population of higher lying energy levels of thulium. The fiber and laser cavity optimization is discussed as well. Using a comprehensive numerical model of TDF we investigated performance of the proposed laser at around 810 nm in three different hosts: fluoride glass (ZBLAN), standard silica and silica modified by high alumina codoping. We have confirmed that lasing at 810 nm is more difficult to achieve with silica based TDF in contrast to the fluoride host materials. However, the lasing might be possible even for silica based fiber for specific ranges of the fiber and laser cavity parameters, especially when $^3H_4$ lifetime is enhanced by modification of local environment of the thulium ions by high-alumina codoping. Results of numerical modeling indicate that the output power of the fiber lasers with fluoride-based TDF and the modified silica TDF are even comparable when the TDF and laser cavity parameters are optimized. The predicted output power of the upconversion laser is about 2 W at 810 nm with moderate pump power of 5 W at wavelength of 1064 nm. For measured thulium spectra in the developed host material, the laser tunability of more than 30 nm is expected.

Acknowledgements

The work was supported by CNRS Office of International Relations project No. PICS 5304, Czech Science Foundation project No. P205/11/1840 and by the Ministry of Education, Youth and Sports of the Czech Rep., project No. ME10119 “FILA”. LPMC is with GIS ‘GRIFON’ (CNRS, www.unice.fr/GIS).